Wide-Band Distributed Modeling of Spiral Inductors in RFICs

Adam Watson*, Pascale Francis**, Kyuwoon Hwang** and Andreas Weisshaar*

* Department of Electrical and Computer Engineering
Oregon State University
Corvallis, OR 97331-3211
** National Semiconductor Corporation
Santa Clara, CA 95052

Abstract **— A new wide-band model for planar spiral inductors on silicon substrate consisting of ideal lumped elements is presented. The equivalent circuit model captures the distributed behavior of the spiral for electrically large devices in particular with low self-resonant frequency. A fast, automated extraction procedure is developed for determining the circuit element values from two-port S- parameter data. The new modeling methodology is applied to extract a distributed model from the measured S- parameters of an electrically large 1.5-nH spiral. The extracted model shows excellent agreement with the measured data over a frequency range of 0.1 to 10 GHz.**

I. INTRODUCTION

The use of monolithically integrated on-chip spiral inductors has become commonplace in the RFIC industry. The RFIC design process requires accurate inductor models that can be included in the circuit simulation along with the entire IC design. To be widely usable, the spiral inductor model should have a compact equivalent circuit topology consisting of ideal elements while be able to capture distributed effects for electrically larger spirals.

Various compact equivalent circuit models based on the π network topology shown in Fig.1 have been developed in recent years. These include the commonly used nine-element π network model with series branch $Z_{series}(\omega)$ consisting of a series inductor and resistor together with a parallel-connected capacitor (e.g. [1,2]), and its extension to a wide-band model having transformer loops in the series branch to account for frequency-dependent conductor and substrate loss effects [3]. The limitations of the single π network topology (Fig. 1) become apparent as the physical size of the spiral becomes electrically larger. Distributed effects in the spiral inductor are directly observed as a *decrease* in the effective series branch resistance $R_{12}(\omega)$ at higher frequencies even to *negative* resistance values in the frequency-range of interest, where

$$Z_{series}(\omega) = -\frac{1}{Y_{12}(\omega)} \approx R_{12}(\omega) + j\omega \cdot L_{12}(\omega) \qquad (1)$$

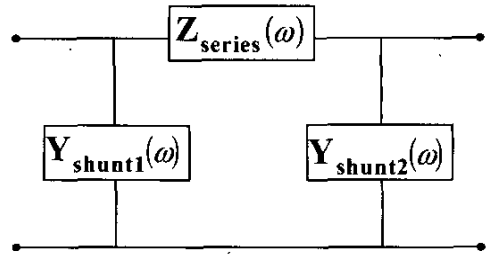

Fig. 1. Standard π network topology for compact spiral inductor models.

and $Y_{12}(\omega)$ is the short-circuit mutual admittance parameter of the two-port network [4]. The decrease in $R_{12}(\omega)$ to negative values cannot be represented by the branch series impedance element $Z_{series}(\omega)$ in Fig. 1 with ideal lumped R,L,C elements.

In this paper a new distributed model consisting of two cascaded π network sections (double π network topology) is proposed to accurately represent distributed effects in spiral inductors. The new model consists entirely of ideal elements including transformer loops to capture frequency-dependent conductor and substrate losses. The new distributed modeling methodology further includes a fast, automated extraction procedure to determine the ideal element values of the distributed equivalent circuit model from the two-port S-parameters of the spiral inductor. The new model can accurately reproduce the characteristics of a large class of spiral inductors beyond the first self-resonant frequency. To verify the capabilities of the new model, a sample inductor model is extracted from measurement data.

II. DISTRIBUTED EQUIVALENT CIRCUIT MODEL

To include distributed effects in a compact spiral inductor model, the single π network topology is extended to an equivalent, higher-order ladder network. The resulting double π network model is shown in Fig. 2. The frequency dependent shunt admittance and series impedance branches can be represented over a wide

0-7803-7695-1/03/$17.00 © 2003 IEEE

frequency range by ideal lumped element circuits, similar to the wide-band equivalent circuit model in the single π network topology described in [3]. The corresponding new wide-band distributed equivalent circuit model for spiral inductors is shown in Fig. 3. Each shunt branch is modeled as standard C-GC circuit to represent the electrical interactions with the Si-SiO_2 substrate. The resulting shunt admittances are given by

$$Y_{shunt,i}(\omega) = \frac{j\omega \cdot C_{ox,i} \cdot (G_{sub,i} + j\omega \cdot C_{sub,i})}{G_{sub,i} + j\omega \cdot (C_{ox,i} + C_{sub,i})} \quad (i = 1,...3) \tag{2}$$

The series branches model the resistance and inductance of the metal windings of the spiral. To model the frequency dependence of the series branches, transformer loops are utilized, as presented in [6]. An additional parallel capacitance is added to include the capacitive effects between the metal windings of the spiral inductor. Interwinding capacitance has increased importance when capturing the distributed characteristics of the metal windings. The frequency dependence in the series branches can be described by

$$Z_{series}(\omega) = \frac{1}{j\omega \cdot C_w + \dfrac{1}{R_{dc} + j\omega \cdot L_{dc} + \dfrac{\omega^2 \cdot M_s^{\,2}}{R_s + j\omega \cdot L_s}}} \tag{3}$$

The transformer loops model the effects of frequency-dependent series loss in the spiral inductor, which can be attributed primarily to conductor skin and proximity effects as well as substrate eddy-current loss for low-resistivity substrates [3,6]. The general trend of these loss mechanisms is an increase in series resistance and a decrease in series inductance with increasing frequency. Distributed effects resulting in a decreasing or negative effective series resistance $R_{12}(\omega)$ at higher frequencies are obtained in the new distributed equivalent circuit model through the interaction of the series and center shunt branch circuits.

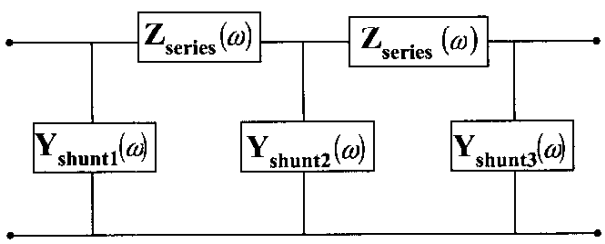

Fig. 2. Distributed double π network topology.

III. Extraction Procedure

An important part of our modeling methodology is the fast and accurate extraction of the component values for the equivalent circuit model shown in Fig. 3. Here the extraction procedure comprises two steps. In the first step, the branch impedance and admittance functions are determined from the two-port network parameters in closed form. Then each branch is synthesized separately in terms of ideal element circuits as described below.

In the first step, the four branch functions of the distributed double π network shown in Fig. 2 are determined from the two-port short-circuit admittance parameters expressed as

$$Y_{11}(\omega) = Y_{shunt1}(\omega) + \frac{Y_{shunt2}(\omega) + \dfrac{1}{Z_{series}(\omega)}}{2 + Z_{series}(\omega) \cdot Y_{shunt2}(\omega)} \tag{4}$$

$$Y_{12}(\omega) = -\frac{1}{Z_{series}(\omega) \cdot (2 + Z_{series}(\omega) \cdot Y_{shunt2}(\omega))} \tag{5}$$

$$Y_{21}(\omega) = Y_{12}(\omega) \tag{6}$$

$$Y_{22}(\omega) = Y_{11}(\omega) - Y_{shunt1}(\omega) + Y_{shunt3}(\omega) \tag{7}$$

Since a reciprocal two-port network has only three independent network parameters [4], a fourth independent relationship must be invoked. Here we assume the admittance $Y_{shunt2}(\omega)$ of the center branch to be a scaled version of the average admittance of the two outer shunt branches.

By adding a center shunt branch, the negative resistance trends in the overall series resistance parameter $R_{12}(\omega)$ can be achieved while the individual branch functions can be synthesized in terms of ideal lumped elements. In order to use the synthesis method in [7], the interwinding capacitance is first extracted from $Z_{series}(\omega)$ as

$$Z_{RL}(\omega) = \frac{1}{\dfrac{1}{Z_{series}(\omega)} - j\omega \cdot C_w} \tag{8}$$

The resulting impedance function $Z_{RL}(\omega)$ represents a monotonically increasing resistance and monotonically decreasing inductance which can be synthesized using Cauchy's method [8] as described in [7]. Similarly, the shunt admittance functions can be synthesized in terms of C-GC circuits [7]. The overall extraction process produces an equivalent circuit with frequency independent lumped

elements, which directly enables simulation in the frequency or time domain. Typically a complete model is extracted in less than 90 seconds on a standard Sparc Ultra10 workstation using the presented method.

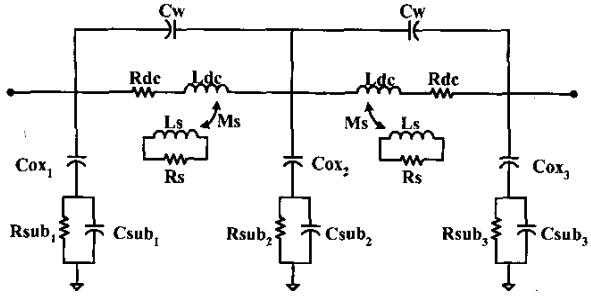

Fig. 3. New wide band distributed equivalent circuit model for spiral inductors in RFICs.

IV. Results

A sample extraction was performed for a large octagonal, 3 turn, 1.5-nH spiral inductor fabricated in a BiCMOS process with bulk substrate resistivity of about $10\ \Omega\cdot\mathrm{cm}$. The new double π model was extracted using single transformer loop series branches and C-GC shunt branches. Table 1 lists the extracted circuit component values obtained with the automated extraction procedure described above. The model results for the series resistance parameter $R_{12}(\omega)$ defined in (1) are shown in Fig. 4. The curve for $R_{12}(\omega)$ obtained with the extracted distributed model is in good agreement with the measurement data. The series resistance parameter can achieve negative values because of the presence of the additional shunt C-GC branch at the center. In contrast, the single π model with transformer loops cannot reproduce the distributed trends in $R_{12}(\omega)$. Curves for $L_{12}(\omega)$, as defined in (1), are shown in Fig. 5. The model results are in excellent agreement with the corresponding measurement data. To further demonstrate the accuracy of the new distributed model over a wide range of frequencies, the input quality factor $Q_{11}(\omega)$ defined as

$$Q_{11}(\omega)=\frac{\mathrm{Im}\left(\frac{1}{Y_{11}(\omega)}\right)}{\mathrm{Re}\left(\frac{1}{Y_{11}(\omega)}\right)} \qquad (9)$$

was calculated. To illustrate the improvement of the new double π model in comparison with currently available techniques the results for the single π model with transformer loops [7] are also included. A comparison plot of $Q_{11}(\omega)$ is shown in Fig. 6. The new double π model produces a significant improvement in matching $Q_{11}(\omega)$ compared with the single π model. The relative error of $Q_{11}(\omega)$ for the new double π model over the entire frequency range is approximately 3.5 % in comparison with 16.4 % for the single π model.

TABLE 1:

EXTRACTED CIRCUIT PARAMETERS FOR A 1.5-NH SPIRAL

Parameters	Extracted Value
R_{dc}	0.432 Ω
L_{dc}	0.684 nH
M_s	6.475 nH
L_s	1.000 μH (arbitrary scaling factor)
R_s	10.19 $K\Omega$
C_w	28.29 fF
C_{ox1}	4.177 fF
C_{sub1}	2.387 fF
R_{sub1}	4.481 $K\Omega$
C_{ox2}	92.42 fF
C_{sub2}	220.3 Ω
R_{sub2}	50.65 fF
C_{ox3}	4.236 fF
C_{sub3}	2.202 fF
R_{sub3}	5.265 $K\Omega$

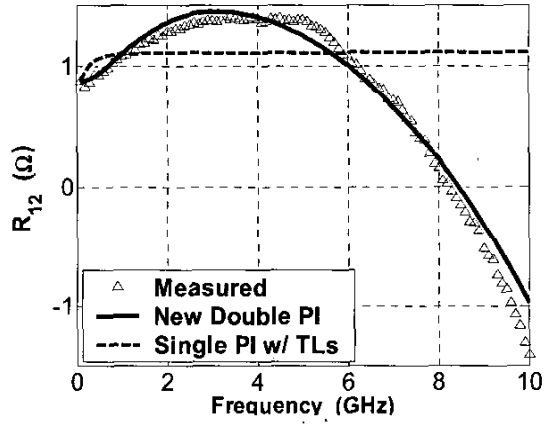

Fig. 4. Series $R_{12}(\omega)$ for measurements, new distributed equivalent circuit model, and wide-band single π model with transformer loops (TL) [7].

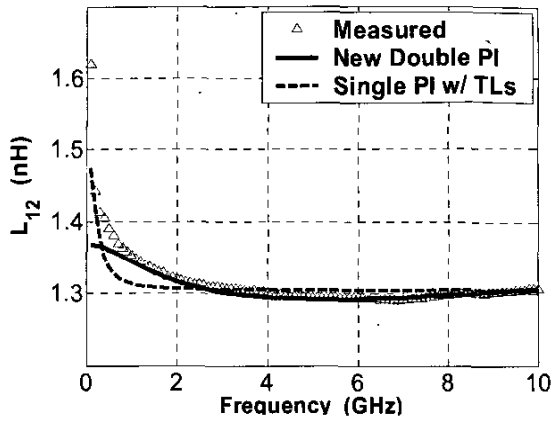

Fig. 5. Series $L_{12}(\omega)$ for measurements, new distributed equivalent circuit model, and wide band single π model with transformer loops (TL) [7].

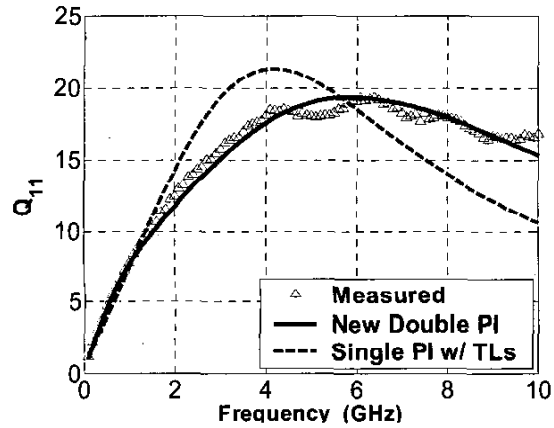

Fig. 6. Quality factor $Q_{11}(\omega)$ obtained from measurements, new distributed (double π) model, and wide-band single π model with transformer loops (TL) [7].

V. CONCLUSION

A new distributed wide-band equivalent circuit model was presented for the characterization of electrically large spiral inductors. A comprehensive methodology for parameter extraction was developed that expands on currently available techniques. The extraction process is considerably faster in comparison with standard optimization techniques. To verify the accuracy of the new methodology, a sample model was extracted from two-port S-parameter measurements for a 1.5-nH spiral inductor. Results were presented and compared with a wide-band single π model with transformer loops showing a significant improvement in modeling performance. The presented modeling methodology has been tested for a wide range of spiral inductors with varying geometry and process parameters including low resistivity substrates to ensure modeling flexibility. The new wide-band distributed model and corresponding extraction process should be useful for accurate characterization of a large class of on-chip spiral inductors for RF and mixed signal applications. The methodology produces an equivalent circuit with ideal lumped elements allowing for direct implementation of the model in common circuit simulators such as SPICE.

ACKNOWLEDGEMENT

The authors wish to acknowledge helpful discussions with Daniel Melendy.

REFERENCES

[1] J. R. Long and M. A. Copeland, "The Modeling, Design, and Characterization of Monolithic Inductors for Silicon RF IC's," *IEEE J. Solid-State Circuits*, vol. 32, pp. 357-368, Mar. 1997.

[2] S.S. Mohan, M.d.M. Hershensen, S.P. Boyd, and T.H. Lee, "Simple Accurate Expressions for Planar Spiral Inductors," *IEEE J. Solid-State Circuits*, vol. 34, pp. 1419-1424, Oct. 1999.

[3] D. Melendy, P. Francis, C. Pichler, K. Hwang, G. Srinivasan, and A. Weisshaar, "A New Wide-Band Compact Model for Spiral Inductors in RFICs," *IEEE Electron Device Lett.*, vol 23, pp. 273-275.

[4] D. M. Pozar, Microwave Engineering, 2nd Ed. John Wiley and Sons, 1998.

[5] J. N. Burghartz, D. C. Edelstein, K. A. Jenkins, and Y. H. Kwark, "Spiral Inductors and Transmission Lines in Silicon Technology Using Copper-Damascene Interconnects and Low-Loss Substrates," *IEEE Trans. Microwave Theory Tech.*, vol. 45, pp.1961-1968, Oct. 1997.

[6] J. Zheng, V. K. Tripathi, and A. Weisshaar, "Characterization and Modeling of Multiple Coupled On-Chip Interconnects on Silicon Substrate," *IEEE Trans. Microwave Theory Tech.*, vol. 49, pp. 1733-1739, Oct. 2001.

[7] D. Melendy, P. Francis, C. Pichler, K. Hwang, G. Srinivasan, and A. Weisshaar, "Wide Band Compact Modeling of Spiral Inductors in RFICs," *IEEE MTT-S International Microwave Symposium Digest*, pp. 717-720, June 2002.

[8] E.C. Levy, "Complex-Curve Fitting," *IRE Trans. Automatic Control*, vol. 4, pp. 37-43, May 1959.